THE JOURNAL OF GEOLOGY

March 1989

FORMATION AND DIAGENESIS OF WEATHERING PROFILES[1]

H. W. NESBITT AND G. M. YOUNG

Dept. of Geology, University of Western Ontario, London, N6A 5B7 Canada

ABSTRACT

Weathering reactions mainly involve the transformation of feldspars, phyllosilicates, amphiboles, pyroxenes, and volcanic glass to the secondary mineral groups, kandites, illites, smectites, vermiculites, and/or chlorites. Although mineralogical changes are complex, bulk compositional changes to weathering profiles, resulting from chemical weathering, are simple and predictable from kinetic, thermodynamic, and mass balance considerations. Predicted bulk compositional changes are corroborated by studies of Recent weathering profiles developed on a variety of plutonic and volcanic rocks under different climatic regimes. Unlike the mineralogical compositions of profiles, the bulk compositional trends are not noticeably modified by climate; consequently, the simple, predictable bulk compositional trends observed in recent profiles provide a "norm" to which ancient weathering profiles can be compared. *Early diagenetic* reactions may occur prior to burial of the profile by reaction of groundwaters with secondary weathering products. These often result in abnormally high accumulations of Si, CO_2, Ca, and Mg to form clay minerals (smectites) and carbonates. The accumulations may be used as indicators of (paleo-)water tables. *Late diagenetic* reactions occur during and following burial through reaction of basin waters, trapped seawater, or brines with minerals of profiles. Metasomatism is common and includes production of illites, smectites, and chlorites at the expense of kaolinite and reconstitution of partially degraded feldspars to form potash feldspar and albite. Reaction with seawater (high Na/K and Mg/K) results in Na- and Mg-metasomatism, yielding albite and chlorite at the expense of partially degraded feldspars and clay minerals. In contrast, K-metasomatism of buried weathering profiles is favored around the periphery of subsiding continental sedimentary basins where dilute continental ground waters display low Na/K values. NaCl-rich brines and high temperatures in the deep central parts of basins favor the formation of albite at the expense of K-feldspar.

INTRODUCTION

Paleosols have been studied for many years (Wahlstrom 1948; Rankama 1955), and recently there has been a concerted effort to extract from such weathering profiles information about the ancient hydrosphere and atmosphere (Gay and Grandstaff 1980; Schau and Henderson 1983; Holland 1984; Feakes and Retallack 1988). However, more information is required concerning recent profiles before ancient ones can be adequately interpreted. Here, mineralogical and analytical

data, together with thermodynamic and kinetic aspects, are used in an attempt to understand changes in the major element compositions of weathering profiles during their formation. This information can then be used to differentiate the effects of weathering from subsequent processes, such as diagenesis and metasomatism, which are common in ancient weathering profiles.

Nomenclature.—The term *chemical weathering* is restricted to the interactions between waters derived directly from precipitation (generally rain water containing inorganic and organic acids derived from decay of litter in the soil zone) and rocks and their weathering residues. A more detailed discussion is given by Nesbitt and Young (1984). The definition excludes reactions between permanent or perched ground waters and

129

rocks (or residues). The term *weathering solutions* is restricted to the rain water-derived solutions discussed above. Interactions between *ground waters,* rocks, and the materials of the weathering profile are considered to be diagenetic. Only recent profiles formed in well-drained areas (well above the water table) are studied. Similarly, profiles containing evidence of physical modification—e.g., transportation of fine-grained weathering products to the lower part of the profile—are excluded. Exclusion of many profiles is necessary to ensure that observed chemical changes are due solely to chemical weathering processes. For definitions of additional terms such as zone of incipient, intermediate, and mature weathering and primitive, evolved, and mature weathering solutions, see Nesbitt and Young (1984, p. 1526).

The Weathering of some Common Rock-forming Minerals.—Plagioclase is the most abundant mineral of the exposed, unweathered, continental crust (Nesbitt and Young 1984) and among the more rapidly weathered silicates (Garrels and Mackenzie 1967; Grant 1963). Experiments by Busenberg and Clemency (1976) and petrographic and XRD studies (Wahlstrom 1948; Lovering 1959; Meunier and Velde 1976; Markovics 1977; Nesbitt 1979, Nesbitt et al. 1980) indicate that, during weathering, large amounts of kandites (kaolinite-group minerals) ultimately are produced at the expense of plagioclase. The Stone Mountain granite in Georgia (Grant 1963) is a typical example. In figure 1 the modal analyses for the Stone Mountain profile are recast and plotted against the Chemical Index of Alteration (CIA), which is a measure of the degree of weathering (Nesbitt and Young 1982, 1984). An antipathetic relationship exists between plagioclase and kaolinite, as expected if plagioclase alters to kandites. The changing proportion of plagioclase and secondary clay minerals are reflected in the CIA values (abscissa). It increases from approximately 55 (CIA values of feldspars and biotite = 50) to 80. (The CIA value of illite is approximately 75 and kaolinite is 100.)

Potassium feldspars apparently weather more slowly than plagioclase (Busenberg and Clemency 1976; Nesbitt and Young 1984), and this is apparent in figure 1. Subequal amounts of plagioclase and potash feldspar are present in the fresh Stone Mountain gran-
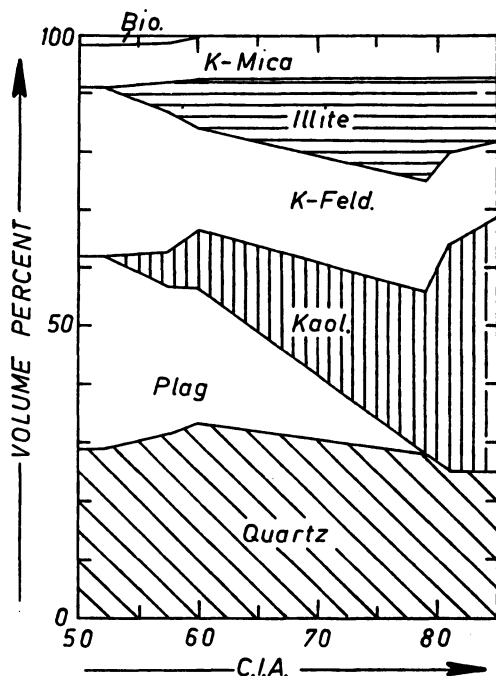

Fig. 1.—Changes in the volume percentages of minerals (ordinate) as a function of weathering intensity (measured by CIA, see Nesbitt and Young 1982, 1984) in the Stone Mountain weathering profile (Georgia, USA). Data are recalculated from results given by Grant (1963, fig. 1), and CIA values were calculated by noting the proportions of minerals and their respective CIA values (feldspars and biotite = 50; muscovite and illite = 75; kaolinite = 100).

ite, but plagioclase is completely altered in the more weathered part of the profile, whereas K-feldspar remains in the most weathered sample (CIA = 85). Busenberg and Clemency (1976), Weaver (1967), and Weaver and Pollard (1973, p. 7–19) concluded that illite is a common alteration product of K-feldspar. Illites form during the weathering of granite rocks (Brock 1943; Wahlstrom 1948; Sand and Bates 1953; Grant 1963; Nesbitt et al. 1980) and mass balance considerations (source of K), coupled with the antipathetic relationship between K-feldspar content and the amount of illite produced in situ (fig. 1), require the illite to be derived from weathering of K-feldspar.

There are numerous experiments and field studies of phyllosilicate weathering. Biotite and chlorite commonly weather to vermiculite (e.g., Wahlstrom 1971), but kaolinite and
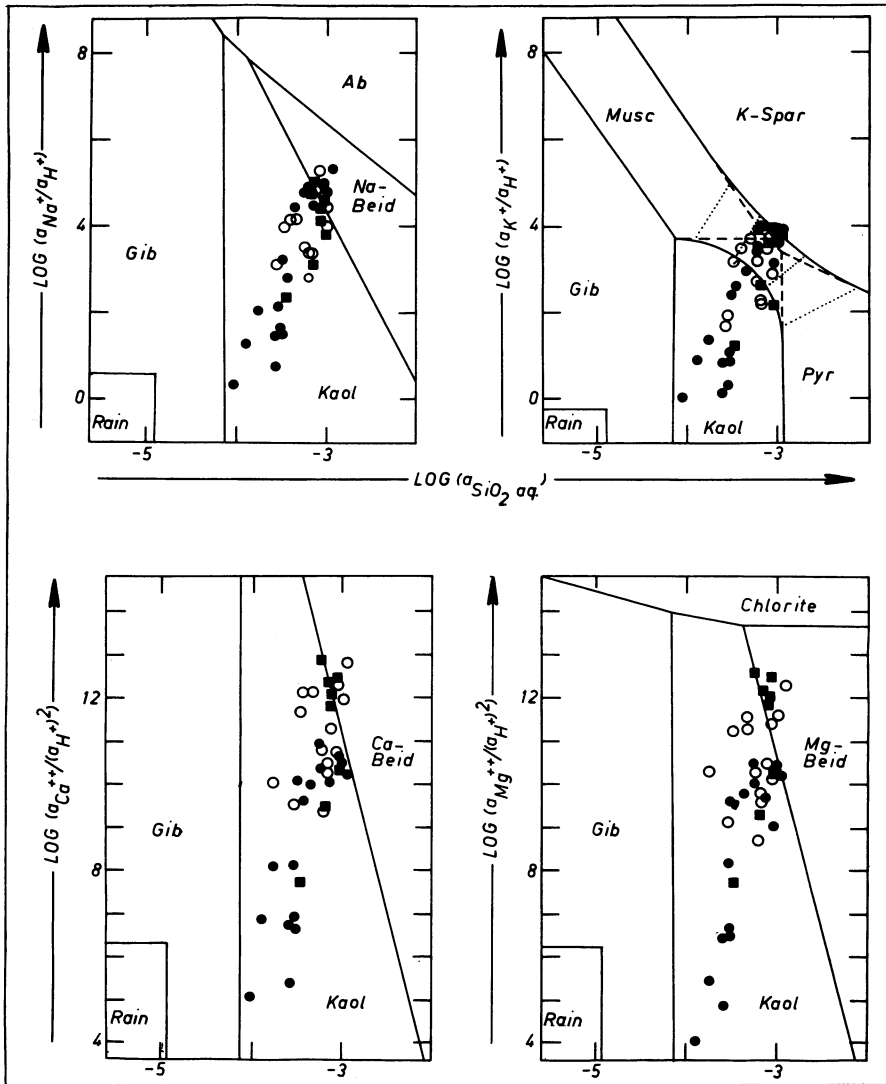
Fig. 2.—Important thermodynamic stability relations between some common minerals, weathering solutions, and shallow ground waters (thermodynamic data from Nesbitt 1977; Helgeson 1969). Waters from granitic and rhyolitic waters (circles) and from basaltic and gabbroic terrain (squares) are taken from White et al. (1963, tables 1 and 2 respectively). The dots represent waters from granitic and weathered granitic terrain (Paces 1972). The dotted curves denote the illite stability field, the composition of which is $K_nAl_2(Si_{4-n}Al_n)O_{10}(OH)_2$ where n may vary between 0 and 1, as indicated by the numbers associated with the dotted lines. The dashed lines are metastable extensions of stability field boundaries. Gib = gibbsite; Kaol = kaolinite; Beid = smectite (beidellite component); Pyr = pyrophyllite; Musc = muscovite; Ab = albite; K-feldspar = microcline.

smectite are also reported (Tsawlassou 1971; Clauer 1981). Muscovite may remain unaltered during the incipient stage of weathering (Meunier and Velde 1976). When it is in contact with plagioclase or biotite, however, it may be replaced by kaolinite. Degradation of the bulk of muscovite probably occurs during the more advanced stages of weathering.

Waters associated with incipient and intermediate stages of weathering (defined by Nesbitt and Young 1984) plot, respectively, at the illite-K-feldspar boundary and within the stability fields of illite and smectite (fig. 2 and Nesbitt and Young 1984). During advanced stages, aggressive weathering solutions should react with these phases to pro-
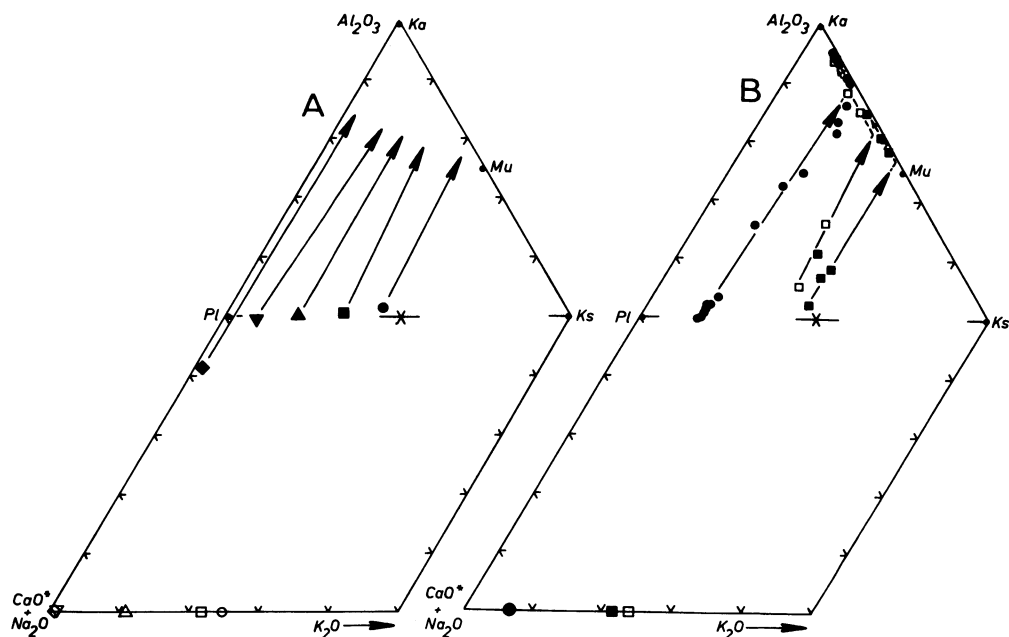
FIG. 3.—Calculated and actual weathering trends of some crystalline rocks (MOLAR PROPORTIONS) are plotted. Small dots are idealized mineral compositions. CaO* represents CaO associated with the silicate fraction of the sample (see Nesbitt and Young, 1982 for details of the calculation). Pl = plagioclase; Ks = alkali feldspar; Mu = muscovite; Ka = kaolinite. The large dot in 3A represents average granite, the square represents average adamellite, the triangle average granodiorite, the inverted triangle average tonalite, and the diamond represents average gabbro. In 3B filled squares, open squares, and dots are fresh and weathered materials from the Stone Mountain Granite, Mazaruni Granite, and Toorongo Granodiorite profiles respectively. The calculated proportions of Ca, Na, and K in leachants (derived from rock with corresponding symbol) are plotted on the baselines of the two triangles. The arrows are the calculated initial trends followed by the leachates during the initial weathering stages. The dashed arrows mimic the advanced trends of the weathering products.

duce kaolinite and/or gibbsite (Meunier and Velde 1976; Grant 1963). Nesbitt and Young discuss in detail the stages of weathering.

THE A-CN-K AND A-CNK-FM DIAGRAMS

Nesbitt and Young (1984) successfully predicted weathering trends for a variety of igneous rocks using kinetic data for feldspar dissolution. On figure 3A are plotted the bulk compositions of average gabbro, tonalite, granodiorite, adamellite, and granite (solid symbols). Included in figure 3A (open symbols at base) are the calculated (using kinetic data) compositions of weathering solutions removed from each of the unweathered rocks during the initial stages of weathering (Nesbitt and Young 1984). Mass balance restrictions require that the compositional trends of the weathered residues plot on a line emanating from each fresh rock and directed away from the respective solution composition. The arrows of figure 3A illustrate these predicted residual weathering trends for each of the average rock types. Bulk compositions of samples taken from the weathering profiles developed on the Toorongo Granodiorite, Mazaruni Granite, and the Stone Mountain Granite are plotted on figure 3B (dots, open squares, and solid squares respectively). Compositions of the initial weathering solutions (calculated using kinetic data for feldspars) are also plotted on figure 3B (along base), as are the calculated weathering trends (arrows) for each profile (see Nesbitt and Young 1984 for details of calculation). The calculated trends mimic the actual trends, indicating that initial weathering trends can be predicted for granites and granodiorites using the kinetic leach-rate data for alkalis and Ca from feldspars.

A second diagram (fig. 4) is introduced to illustrate the relationship between leucocratic and melanocratic constituents in weathering profiles. CaO*, Na_2O, and K_2O are summed
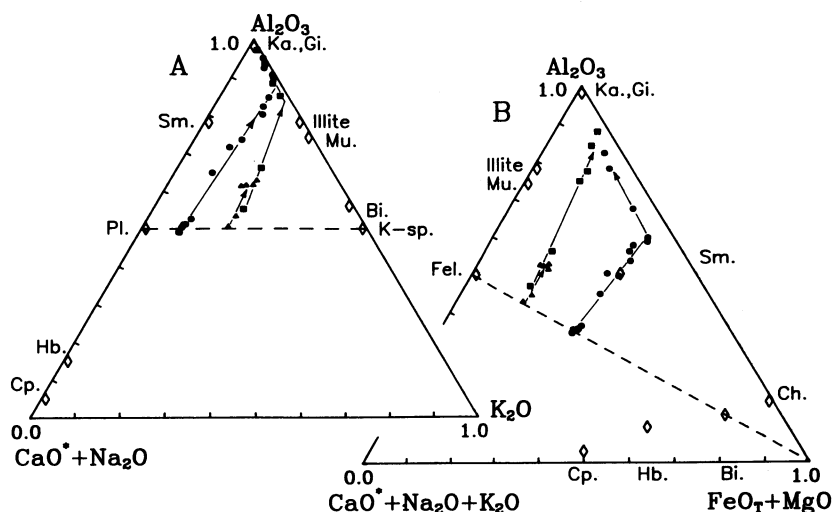
Fig. 4.—Weathering trends for the Mazaruni Granite profile (squares), the Ricany Granite profile (triangles), and the Toorongo Granodiorite profile (dots) are shown. The arrows in 4A (A-CN-K diagram) have been calculated from feldspar leach rate data. The arrows of 4B (A-CNK-FM diagram) are drawn to reflect the plotted data only. The diamonds represent idealized mineral compositions; Sm = smectite (montmorillonites and beidellites); Il = illite (sericites, phengites, celadonites); Bi = biotite; Fs = feldspars (plagioclase and K-feldspar). See figure 3 for other abbreviations. These triangular plots and all subsequent triangular plots are as MOLAR PROPORTIONS

and plotted at the lower left apex, Al_2O_3 at the top, and FeO (total iron as FeO) and MgO are summed to form the third variable. The diagram is referred to as the A-CNK-FM diagram (fig. 4B). It is similar to the ACF diagram used in metamorphic petrology. Weathering trends cannot be calculated for this diagram because the requisite kinetic data are not yet available, but some generalizations based on mineralogical and mass balance arguments can be made. The rate of weathering of biotite is similar to the rate of Na removal from plagioclase of the Toorongo and Boulder Creek Granodiorites (Nesbitt and Young 1984). If this relationship holds generally, and plagioclase and biotite are the major leucocratic and melanocratic minerals of the parent rock, a simple, regular compositional trend should be produced in A-CNK-FM space. Only when the proportion of the one mineral changes dramatically (i.e., when completely weathered) should the bulk compositional trends display abrupt changes in direction.

COMPOSITIONAL TRENDS IN RECENT
WEATHERING PROFILES

Granites and Granodiorites.—The Toorongo Granodiorite (Markovics 1977; Nes-

bitt et al. 1980) is situated in a mountainous cool temperate climate (Victorian Alps, Australia) with moderate rainfall (approx. 80 cm/yr). The bulk composition of the fresh granodiorite and weathered samples from the profile are plotted on figure 4A (dots). As discussed in the previous section, the observed initial trend (figs. 3B and 4A, dots) and the calculated trend coincide, confirming that plagioclase is weathered rapidly (see also fig. 1). Continued weathering results in progressive destruction of plagioclase, eventually to the point where little Ca or Na remains in the residue (in either plagioclase or secondary products). For this situation, the bulk compositions of the residues plot close to the A-K join. Since residues plotting along the A-K join contain little Ca- or Na-bearing phases, the dominant minerals that remain are aluminous phases such as kaolinite and potassic phases such as illite and/or K-feldspar (fig. 1). Once bulk compositional trends approach the A-K join, they are redirected toward the Al_2O_3 apex (fig. 4A); apparently, incongruent dissolution of the potassic phases releases K to solution in preference to Al so that the trend in bulk composition is toward the Al_2O_3 apex (fig. 4A).

The bulk compositions of samples from the

Toorongo profile are also plotted on figure 4B (dots). The initial trend (early weathering) is sub-parallel to the A-CNK boundary of the triangle. Once the A-FM boundary is approached (advanced weathering) there is an abrupt change in the weathering trend toward the Al_2O_3 apex. Apparently $Fe_T + Mg$ are leached from the residual products more rapidly than is Al_2O_3.

The Mazaruni Granite (Lovering 1959) is located in a tropical, very high rainfall region of British Guiana. The initial trend (figs. 3A, 4A, squares) shows that Ca and Na are extracted from the granite in preference to K (in an approx. 2:1 proportion). The weathering trend of the fresh granite has been calculated from kinetic data (Nesbitt and Young 1984) and conforms closely to the observed bulk compositional trend (fig. 3A, arrow associated with the squares). Progressive chemical weathering destroys plagioclase rapidly (fig. 1), and the bulk compositions of the residues evolve toward the Al-K join. As the join is approached, little Ca or Na remain and, in the compositional space of figure 4A, only potassic (e.g., K-feldspar, illite) and aluminous phases (e.g., kaolinite) remain to be weathered. The Mazaruni weathering trend changes abruptly at the A-K join and is redirected toward the Al_2O_3 apex. It is apparent that potassium has been extracted from the profile more rapidly than has Al. In the A-CNK-FM diagram (fig. 4B), the Mazaruni data define a trend sub-parallel to the A-CNK join, suggesting that the weathering solutions extracted $CaO + Na_2O + K_2O$ and $FeO_T + MgO$ from the granite in a ratio approximately equal to that found in the fresh granite.

Although the Mazaruni Granite is compositionally different from the Toorongo Granodiorite (fresh rocks plot in different positions on fig. 4A and 4B), their trends are qualitatively similar.

The Ricany Granite (Minarik et al. 1983) is part of the Bohemian Massif (Czechoslovakia), situated in a temperate climate. The bulk composition of the fresh granite (fig. 4A, triangle plotting closest to the feldspar join) is similar to fresh Mazaruni Granite. Also, the bulk compositions of the weathered samples define an Al-enrichment trend that is sub-parallel to the right-hand boundary of the A-CNK-FM triangle (fig. 4A) and sensibly the

same as the trend for the Mazaruni profile. The Ricany Granite is compositionally similar to the Mazaruni Granite in A-CNK-FM space, and the two trends are again sensibly the same. The two fresh granites are compositionally similar, and the weathering trends are also similar, although the climatic conditions of weathering are different.

The Stone Mountain Granite weathering profile (Georgia, USA) formed in a warm temperate climate. The mineralogical data (fig. 1) of Grant (1963) (fig. 3B, stars) have been recast into bulk compositions, and the data for fresh and weathered samples plotted on figure 3A. The initial trend is sub-parallel to the A-CN join and is similar to the trend calculated using kinetic data for leaching of alkalis and Ca from feldspars (Nesbitt and Young 1984). There is an abrupt change in the weathering trend at the A-K join, and it is redirected toward the Al_2O_3 apex. The trends for the granites and granodiorites are similar, regardless of bulk or mineralogical composition.

Tonalites and Gabbros.—There are no published, complete major element analyses of weathering profiles developed on tonalites or gabbros where sampling was sufficiently detailed to include analyses from each of the weathering zones. These rocks contain abundant CaO and only small amounts of K_2O; hence they plot close to the A-CN boundary. The compositional trends developed during chemical weathering have been calculated (fig. 3A; see Nesbitt and Young 1984 for details of calculations). The calculations indicate that the weathering trends are sub-parallel to the A-CN boundary, but closer to the boundary than are the trends for the more potassic rocks of figure 3A. As a result, the gabbro and tonalite weathering trends are directed toward the smectite and kaolinite fields, and these phases are expected to form in quantity, either directly from primary minerals, or after other intermediate products. Much less illite is expected to form in these profiles compared with amounts found in granitic and granodioritic profiles because of the bulk compositional restrictions.

Weathering trends of gabbros and tonalites in A-CNK-FM compositional space (fig. 4B) cannot be calculated because insufficient experimental kinetic data exist. Mineralogical arguments, therefore, are used to predict
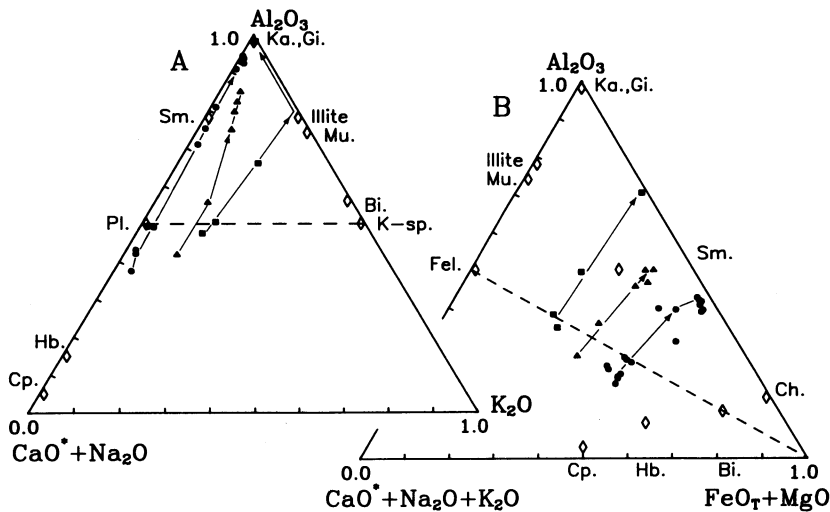
Fig. 5.—Weathering trends for the Baynton Basalt (dots), the Kiama Latite (triangles) and the Tai Mo Shan Rhyolite (squares). The initial weathering trend is calculated for the rhyolite in 5A (A-CN-K diagram) but all other arrows reflect compositional trends only (not calculated). Labels and diamonds are as in figure 4.

weathering trends. The weathering trend in A-CNK-FM space includes compositional vectors directed away from the biotite, hornblende, and feldspar compositions (fig. 4B) because these are destroyed during weathering. The magnitudes of the vectors are uncertain. There are also compositional vectors directed toward the authigenic phases (kaolinite, smectites, illites, etc.) and the magnitudes of the vectors are determined by the amounts produced. The plagioclase weathering vector emanates from the bulk composition of the unweathered parent rock and is directed away from the feldspar composition, whereas the vector corresponding to kaolinite production, for example, emanates from the bulk composition toward kaolinite composition (Al_2O_3 apex); consequently, the resultant vector is directed toward the $(FeO + MgO) - Al_2O_3$ boundary. Since plagioclase is the most abundant mineral of most tonalites and gabbros, the resultant vector will be most affected by the weathering of this feldspar.

The biotite and hornblende vectors also influence the resultant vector, and their effects are uncertain. Fortunately, the primary mineralogy of many diorites and gabbros is similar to that of the Toorongo granodiorite, and we anticipate that the weathering trends will be sub-parallel to the Toorongo trend.

Other diorites and gabbros contain abundant hornblende and/or pyroxenes, and their weathering trends may be different from the Toorongo trend.

Volcanic Rocks.—Brock (1943) reports data for the Tai Mo Shan rhyolite porphyry (fig. 5A, squares). The initial weathering trend is sub-parallel to the left boundary. White (1983) provides experimental Ca, Na, and K leach rates for rhyolitic glass, and they are compatible with the trend of the Tai Mo Shan data (fig. 5A, squares), as well as the trends observed for granites (fig. 4A). The analytical and experimental data suggest that, initially, rhyolitic and granitic rocks weather similarly and sub-parallel to the left-hand boundary of figures 4A and 5A.

Trends from the Baynton Basalt (Wilson 1978) and Bumbo Latite (Craig and Loughnan 1964) are sub-parallel to the left boundary in figure 5A. These trends cannot be calculated because there are no experimental leach rate constants available. As for tonalites and gabbros, high concentrations of Mg and Ca in the parent rock, and low concentrations of K, favor the formation of smectites during the initial stages of weathering (fig. 5A). Kandites may form from primary and secondary minerals during the advanced stages of weathering as the bulk composition evolves toward the Al_2O_3 apex. These predictions generally are

observed (Craig and Loughnan 1964; Alt-schuler et al. 1963).

In figure 5B, Ca + Na + K is removed in preference to Fe + Mg, resulting in trends that are sub-parallel to the left boundary. Most likely, Fe and Mg are taken up by smec-tite and oxyhydroxides. Ca may be incorpo-rated into smectite exchange sites, but the amount will be minor compared with the amount present in the fresh basalt.

TEMPLATES FOR WEATHERING OF PLUTONIC AND VOLCANIC ROCKS

The compositional trends of the three gran-ites (Mazaruni, Ricany, and Stone Mountain) and the Toorongo Granodiorite are qualita-tively similar. In figure 3A, the initial trends are sub-parallel to the A-CN join, with a sec-ond segment following the A-K join toward the Al_2O_3 apex. In the A-CNK-FM diagram, the initial trends are also similar. The ability to calculate these initial trends provides added confidence to the conclusion that these trends are *typical* of recent profiles produced by chemical weathering of granites and granodiorites, and probably also tonalites and gabbros. They can be used as templates against which the chemical history of ancient profiles can be read. Deviations from these trends generally are the result of diagenesis and metasomatism. Although compositional trends produced by chemical weathering of volcanic rocks cannot be calculated, the con-sistency of the observed trends indicates that these too can be used as templates for inter-preting ancient profiles.

THE EFFECTS OF CLIMATE ON WEATHERING TRENDS

Singer (1980) and Nesbitt and Young (1984) discuss the effects of climate on weathering profiles and conclude that the extent of weathering is determined primarily by the amounts of acids introduced into the profile by rain water-derived solutions. The Maza-runi weathering profile has formed under tropical conditions where rainfall is 250 to 375 cm yearly (Lovering 1959). The Ricany and Stone Mountain profiles formed in a humid climate of moderate temperature (Minarik et al. 1983; Grant 1963), and the Toorongo Granodiorite profile in a mountainous cool temperate environment of moderate rainfall (approx. 80 cm/yr). The basaltic profiles

shown in figure 6 also formed in different climatic environments. The Morvern basalt profile (Scotland) of figure 6 developed in a cool temperate, humid climate (approx. 180 cm/yr rainfall; Bain et al. 1980), whereas the Baynton profile (Vic. Australia) formed in a warm temperate climate of relatively low rainfall (approx. 50 cm/yr precip.). The Casino profile (northeastern NSW) was formed in a moderately humid (110 cm/yr pre-cip.) sub-tropical climate.

As observed in figures 3B, 4, and 6, the weathering trends of plutonic and volcanic rocks are controlled by the bulk compositions of the parent rocks, and there is no noticeable climatic effect on these trends. We conclude that there is no significant climatic effect on weathering trends within the compositional space represented by these diagrams.

DIAGENESIS OF WEATHERING PROFILES

Weathering reactions are defined to include only reactions between solids and rain-water (acidified during passage through litter and the organic zone of soils) percolating through the profile. The definition excludes reactions with ground waters (solutions below the wa-ter table, perched or regional), formation wa-ters or connate waters, or reactions resulting from other processes. Weathering reactions, by this definition, almost invariably result in removal of constituents from profiles.

Early Diagenetic Reactions.—Near-surface ground waters generally are near-neutral to slightly basic (White et al. 1963) and contain significant quantities of dissolved solids. Various reactions between groundwa-ters and weathering profiles may occur, in-cluding transfer of dissolved constituents from solution to the weathering profile (i.e., metasomatism). These products may be superimposed on previously formed weath-ering products where water tables intersect weathering profiles. We classify reactions be-tween ground waters and weathering profiles as diagenetic reactions and all the products as diagenetic products.

Example of reactions with ground waters. Craig and Loughnan (1964) provide analyses of five basaltic weathering profiles from east-ern Australia. The Murrurundi Profile (NSW, Australia) was the only one saturated with water at the time of sampling and, as they suggest, alteration has occurred under condi-
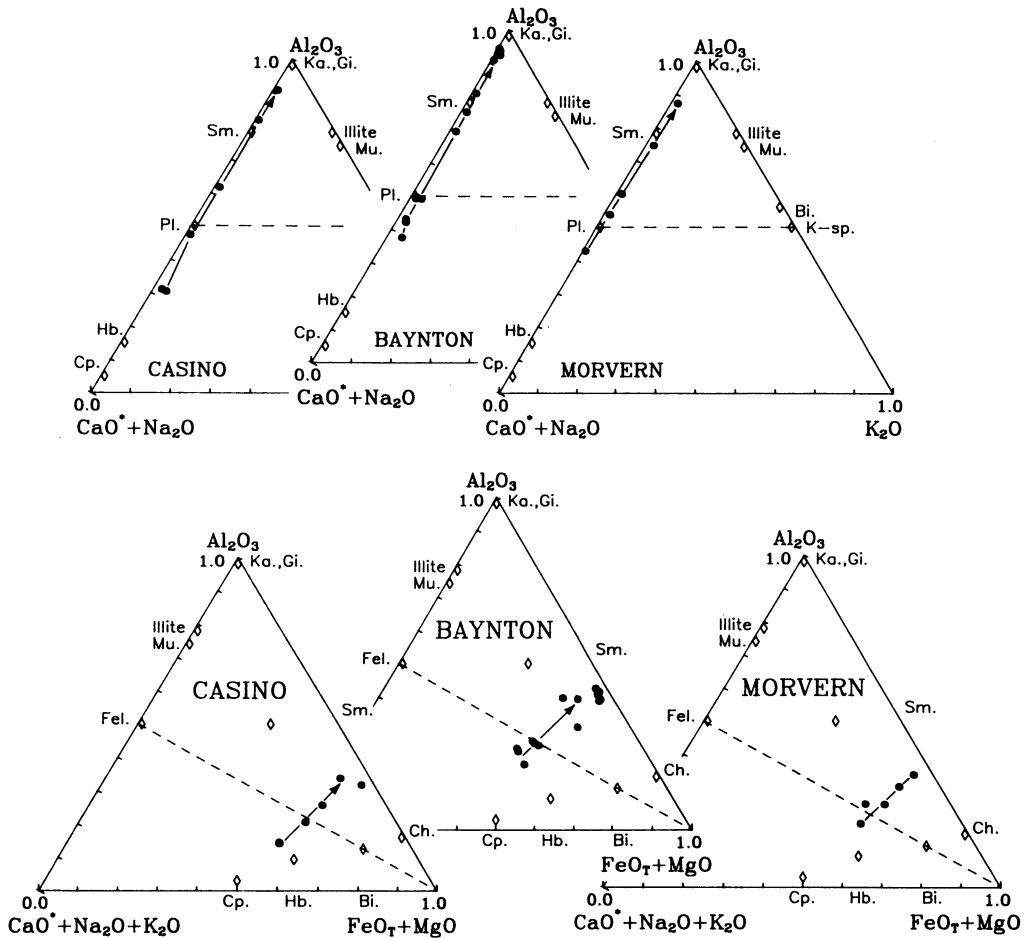
FIG. 6.—Weathering trends of basalts from different climatic zones are shown in A-CN-K and A-CNK-FM compositional space. The Casino profile has developed in a sub-tropical climate (NE NSW, Australia), the Baynton profile in a semi-arid warm temperate climate (central Victoria, Australia) and the Morvern profile has developed in a very humid, cool temperate climate (NE. Scotland). Diamonds and labels are as in figure 4.

tions of impeded drainage, and the water table may be perched. The initial trends in figure 7A and 7B (Murrurundi profile) mimic those of figure 6A and 6B. However, the trend of figure 6B is prematurely redirected upward and toward the left boundary rather than continuing to the right boundary (fig. 7B); hence, in contrast to the other profiles, high proportions of Ca + Na + K remain in the Murrurundi profile. The trend indicates that "atypical" processes affected the Murrurundi profile, and the presence of perched ground waters raises the possibility of reaction between the basalt and the ground waters. There are other anomalies. The zone between 10 and 180 cm ("white plastic clay

zone"; Craig and Loughnan 1964) was saturated when sampled, and compared with fresh basalt, it contains high concentrations of SiO_2, CO_2, Ca, and Mg relative to Ti or Al (fig. 7C). Similar accumulations are absent from well-drained profiles (fig. 6), and we suggest that these constituents have been extracted from the ground waters and deposited in the white plastic clay zone. By our definition these reactions are diagenetic, and the phases containing the deposited elements are early diagenetic products; they mark the position of the water table.

Diagenetic Reactions Resulting from Burial.—Burial diagenesis results from disequilibrium between minerals produced in the
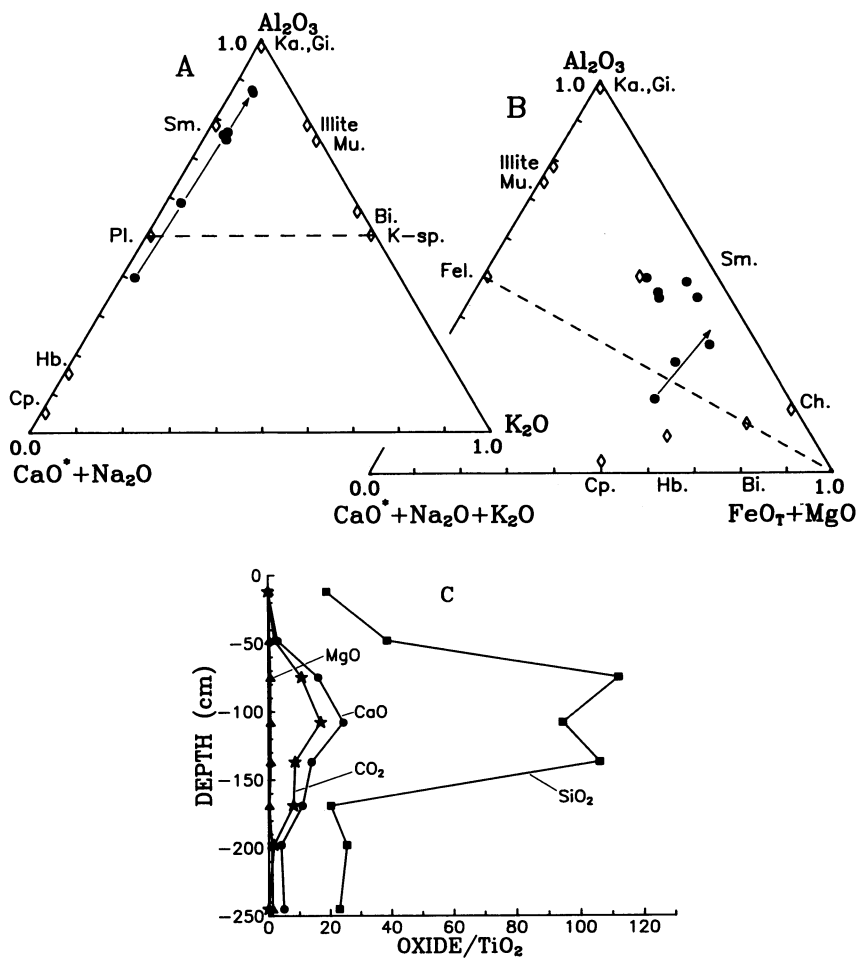
FIG. 7.—Weathering trends for the Murrurundi profile developed on basalt are shown in 7A and 7B. 7C is a section through the profile. It is divided into three zones (Craig and Loughnan 1964). There is a surface zone, an intermediate "white plastic clay" zone (enriched in SiO_2) and below it, resting on fresh basalt, is the third, "much-weathered" zone. The white plastic clay zone is a zone of impeded drainage.

weathering environment and subsurface waters such as formation waters of sedimentary basins. Disequilibrium may result from changes in temperature and pressure and from changes in the chemical environment.

Temperature: The stability fields of kaolinite, muscovite (proxy for illite), and microcline are illustrated in figure 8A as a function of temperature and K^+/H^+ of the equilibrated solutions (1 bar total pressure, water present; data from Helgeson 1969; Nesbitt 1977 for muscovite). K^+/H^+ of waters equilibrated with illite and kaolinite (fig. 2) range from 3.5 to 4. The temperatures of these ground waters range between 10 and 30°C (fig. 8A, solid square). To maintain equi-

librium with illite and kaolinite, K^+/H^+ of the waters must decrease as temperature increases. Considering that Al is conserved in the solids during the reaction, the stoichiometry is:

$$KAl_3Si_3O_{10}(OH)_2 + H^+ + 0.5H_2O = 1.5Al_2Si_2O_5(OH)_4 + K^+. \quad (3)$$
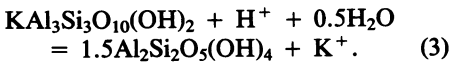
If kaolinite and illite control K^+/H^+ of the waters during burial (and increased temperature), illite would be produced at the expense of kaolinite, causing K^+/H^+ to decrease in solution. If the volume of solution in the intermediate zone were small compared with the mass of solids, the amount of illite formed
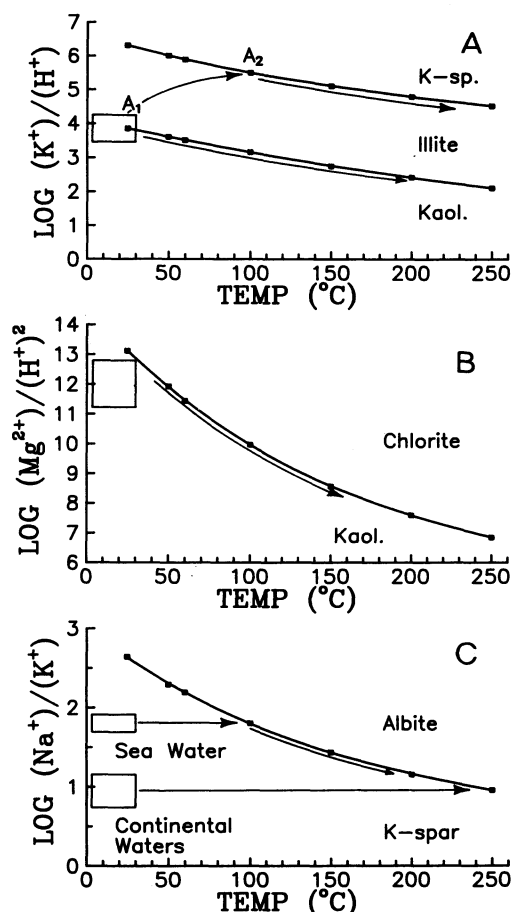
FIG. 8.—Temperature-related changes in ratios of critical species. In 8A, K^+/H^+ values reflecting kaolinite-illite-solution and K-feldspar-illite-quartz-solution equilibria are plotted against temperature. The ratio decreases as temperature increases, reflecting the relative increase in stability of the progressively less hydrated phases at successively higher temperatures. 8B and 8C illustrate kaolinite-chlorite-solution and albite-K-feldspar-solution equilibrium relations as a function of temperature. The boxes of 8A and 8B represent the range of compositions of typical ground waters and sea water.

would be small, but introduction of K^+ by solutions from external sources might result in large quantities of illite being produced, even to the point of destroying all kaolinite.

Reactions may be different elsewhere in the profile. The upper curve of figure 8A illustrates microcline-illite-quartz-solution equilibrium and, as for reaction (3), increasing temperature requires K^+/H^+ to decrease if solutions are to maintain equilibrium with the

two potassic minerals and quartz. When K-feldspar and illite control K^+/H^+ (as they may in the *incipiently weathered zone;* Nesbitt and Young 1984), illite is converted to K-feldspar (eqn. 4) as temperature increases; thus K^+ (aq) and pH tend to decrease:

$$3KAlSi_3O_8 + 2H^+ = KAl_3Si_3O_{10}(OH)_2$$
$$+ 2K^+ + 6SiO_2(aq) \qquad (4)$$
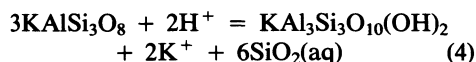
Aqueous silica is involved in the reaction, and the interpretation is correct only when aqueous silica is controlled at or near quartz saturation. The condition probably is met at elevated temperatures and deep burial (Blatt 1979) but not at ambient temperatures, and additional comment is warranted.

Mature weathering solutions (Nesbitt and Young 1984) generally are found in the *zone of incipient weathering* where there exist abundant unweathered primary minerals. These waters are equilibrated with at least one common primary mineral (excluding quartz), generally K-feldspar (Nesbitt and Young 1984). Most are equilibrated with both illite and K-feldspar (plot on the illite-K-feldspar boundary of fig. 2) but are greatly supersaturated with respect to quartz (log $Ksp = -4.00$; Helgeson 1969). As temperature increases, quartz becomes progressively more reactive. Since the solutions are initially supersaturated with respect to quartz, it should precipitate from solution, thus affecting the equilibrium between the solution and the two potassic minerals. As the profile is buried and temperature increases, removal of aqueous silica (quartz precipitation) drives the reaction (eqn. 4) to the right releasing K^+ to solution, replenishing aqueous silica, and consuming H^+. Beginning at point A_1 (fig. 8A, path A), K^+/H^+ may increase as temperature increases (eqn 4) until equilibrium is reached. Once a solution is equilibrated with respect to quartz, illite, and microcline (fig. 8A, point A_2), the subsequent reaction path follows the equilibrium curve: K-feldspar is produced at the expense of illite, quartz is consumed and K^+/H^+ decreases in solution. Additional complications may arise when other reactive silicates are considered.

Mature weathering solutions are undersaturated with respect to albite but saturated with respect to K-feldspar (fig. 2). Partially degraded feldspars, which would be common

in the *incipiently weathered zone* of profiles, normally would be reconstituted to K-feldspar or illite rather than to plagioclase.

Mature weathering solutions are undersaturated with respect to albite but saturated with respect to K-feldspar (fig. 2). Partially degraded feldspars, which would be common in the *incipiently weathered zone* of profiles, normally would be reconstituted to K-feldspar or illite rather than to plagioclase.

The stability fields of chlorite and kaolinite (+ quartz) are shown (fig. 8B) as a function of temperature and $Mg^{2+}/(H^+)^2$. If Al is conserved the reaction between the two is:

$$Mg_5Al_2Si_3O_{10}(OH)_8 + 10H^+$$
$$= Al_2Si_2O_5(OH)_4 + 1SiO_2(c) \qquad (5)$$
$$+ 5Mg^{2+} + 7H_2O.$$
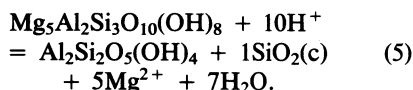
As temperature increases the reaction is forced to the left. Mg is consumed, and if this reaction controls $Mg^{2+}/(H^+)^2$ values during diagenesis then chlorite would form at the expense of kaolinite.

The above reactions proceed as a result of increased temperatures alone. The thermodynamic assessment indicates that illites, degraded feldspars, and possibly plagioclase, may be converted to K-feldspar in the incipiently weathered zones. This is solely the result of increased temperatures, resulting from burial. Kaolinite within the intermediate weathering zone should be converted to illite and chlorite with increased temperatures. These reactions proceed primarily because the less hydrated assemblages become progressively more stable with increased temperatures.

Pressure: Since condensed phases are not easily compressed, the effect of pressure on their free energies of formation is minimal and generally can be disregarded unless there is very deep burial. Although effects of pressure may be significant in some settings (Stephens et al. 1979), they generally are less important than temperature in diagenetic regimes.

Solution compositions: Weathering profiles are porous (Grant 1963) and normally will become saturated with water when buried below the permanent water table. Burial involves introduction of solutes such as potassium which may result in formation of diagenetic illite and/or K-feldspar, as

discussed above. The reactions (K-metasomatism of profiles) probably are common in continental settings. Diagenesis by sea water, saline formation waters or hydrothermal waters may yield different diagenetic assemblages.

Na^+/K^+ of sea water is approximately $10^{1.7}$, and if it were introduced to a weathering profile at approximately 100°C, the water would plot on the albite-K-feldspar boundary (fig. 8C). At higher temperatures, and if kinetically feasible, K-feldspar and illite would be diagenetically altered to albite. Most dilute continental waters have Na^+/K^+ values lower than that of sea water (White et al. 1963; Livingstone 1963), commonly between 3:1 and 15:1. These waters plot within the K-feldspar field for all temperatures below approximately 250°C. Extreme diagenetic or metamorphic conditions are required for albite to form in place of microcline in most weathering profiles if the associated fluids are dilute continental waters. Introduction of sea water, a sea water derivative, or saline Na-rich formation waters may result in the formation of diagenetic albite in buried profiles at relatively low temperatures, well within the range of typical diagenetic conditions (below 200°C).

Calcium may be introduced to the profile to form carbonates or zeolites and possibly some plagioclase. Formation of carbonates or zeolites is unlikely, however, because the "acidic" nature of well developed profiles is not conducive to their formation. Magnesium may be introduced to profiles as carbonate but again the carbonates are unlikely to form during burial. More likely Mg and Fe are introduced as chlorite, the chlorite forming at the expense of kaolinite with Mg and Fe derived from the ground waters.

GEOLOGICAL SETTING AND DIAGENESIS

Diagenesis of profiles may be influenced by regional geological setting. Subsurface waters of most *continental* basins display compositions related to the hydrology of the basin (Habermehl 1980; Lawrence 1975; Hitchon et al. 1971; Graf et al. 1966). The most dilute waters are found in the recharge regions, which generally are around the elevated periphery of the basin, whereas more concentrated waters are found in the deep central portions of basins (Graf et al. 1966). Regional

flow regimes (Toth 1962) include very deep circulation, which is commonly bounded by bedrock below the basin sediments. Weathering profiles on the bedrock may undergo diagenesis when contacted by these deep circulating solutions.

Sea water or a derivative is the common pore fluid in subsiding marine basins, and profiles buried under marine conditions can be expected to suffer Na-metasomatism. Only at low temperatures (T < 100°C) might K-metasomatism occur (fig. 8C) in marine basins, and where temperatures anywhere within the basin exceed approximately 100°C, albite will form in preference to the potassic minerals. In contrast, profiles of continental basins may be subjected to over 200°C without diagenetic albite forming.

The extent of metasomatism of profiles is dependent on the hydrology of the basin and porosity and permeability of the weathering profiles. Porosity and permeability of profiles are generally high (Grant 1963). Rapid decrease in porosity and permeability during burial should preclude such metasomatism. When permeability remains comparable to or higher than the surrounding sediments, the buried profile may act as a basal aquifer with large volumes of fluids migrating through it. Metasomatism then may be extensive and these conditions seem to have prevailed in some of the paleosols now discussed.

APPLICATIONS TO SOME PALEOSOLS

Boulder Creek Profile: Example of Early Diagenesis and Metasomatism.—The Carboniferous Boulder Creek granodiorite is situated west of Boulder, Colorado (Wahlstrom 1948). In the area studied, a fluvial sandstone (Fountain age) unconformably overlies the granodiorite and the paleosol developed from it. The unconformity is of Madison age, and the weathering profile was produced during Carboniferous time (Wahlstrom 1948). The profile extends to a minimum depth of 25 m in the area studied.

Weathering of the granodiorite proceeded along subsurface fractures and joints, leading to the development of "isolated rounded fresh boulders separated by altered matrix" (Wahlstrom 1948). Precisely the same pattern of weathering is observed in recent profiles (Markovics 1977; Nesbitt 1979; Nesbitt et al. 1980). Wahlstrom (1948) notes that

quartz and K-feldspar persisted throughout the profile. Plagioclase weathered more rapidly than did K-feldspar, and biotite and hornblende altered rapidly to vermiculite, iron oxides, and other clay minerals. The same observations are noted at the recent Toorongo Granodiorite profile (Markovics 1977; Nesbitt 1979). Apparently weathering of the Boulder Creek granodiorite during the Carboniferous differs little from recent weathering of the Toorongo Granodiorite.

Anomalies and their explanation: Dolomite is present in the profile from 2 to 18 m above the fresh rock (the bleached zone) as a pseudomorphic product after oligoclase and in veinlets cutting other minerals (Wahlstrom 1948). The distribution of dolomite is restricted, just as is the carbonate of the Recent Murrurundi profile. The dolomite may be an early diagenetic product and its distribution restricted by the location of the water table in the profile.

In the A-CN-K triangle (fig. 9A) the fresh granodiorite plots just below the feldspar join, and the long arrow (sub-parallel to the left boundary) is the initial weathering trend calculated from kinetic data (Nesbitt and Young 1984). All samples plot on the K_2O-rich side of the calculated initial trend, indicating a substantial enrichment in K_2O when compared with either the calculated trend or trends for recent granitic profiles (figs. 3 and 4).

The Carboniferous profile is deep, with three well developed zones (Wahlstrom 1948) indicating a very mature profile. By comparison with the Toorongo Granodiorite profile and other recent profiles developed on granitic rocks, kaolinite should dominate in the highly weathered zone (fig. 1) of the Boulder Creek profile. Kaolinite, however, is scarce and illite is the most abundant clay mineral (Wahlstrom 1948). Wahlstrom (1948) notes that potash feldspar in the bleached zone is devoid of alteration products. In contrast, the K-feldspar of the Toorongo weathering profile is clouded and extensively altered in the intensely weathered portions of the profile. These observations suggest the kaolinite has been converted to illite and K-spar is a diagenetic mineral of the Boulder Creek profile. Apparently there has been pervasive K-metasomatism of the profile. The effects are shown in figure 9A by drawing
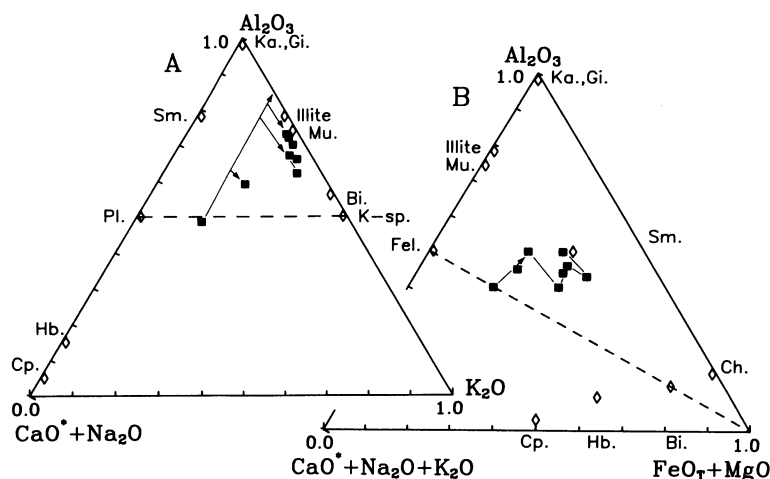
FIG. 9.—Analytical data for a weathering profile developed on the Boulder Creek Granodiorite are plotted on A-CN-K and A-CNK-FM diagrams (data from Wahlstrom 1948). In 9A, the long arrow sub-parallel to the left boundary is the calculated initial weathering trend. The three short arrows directed towards the K_2O apex illustrate the diagenetic changes to portions of the profile that result from K-metasomatism. The arrows of 9B illustrate the erratic trend of the data.

vectors from various points on the predicted weathering trends (long arrow) toward the K_2O apex. Potash addition is pervasive.

None of the data plots close to the Al_2O_3 apices (fig. 9A, 9B). The data of figure 9B plot across the diagram forming an irregular zig-zag pattern. The proportion of Na + Ca + K decreases, but Al does not increase as it does in the recent profiles (fig. 4B). Fe_T + Mg increases relative to the other components of the diagram, and the trend is different from those of recent profiles. Like potassium, Fe + Mg probably was added to the profile during diagenesis through formation of phengitic illite and dolomite and through the reconstitution of micas, possibly at the expense of kaolinite.

Textural evidence indicates that the Boulder Creek profile developed in much the same way as the Toorongo profile. Carbonate probably precipitated early during diagenesis, whereas illite and K-feldspar formed later, during burial of the profile. K- and Mg-Fe-metasomatism affected the compositional trends. Ground waters transported potassium to the profile and, due to increased temperatures associated with burial, kaolinite, degraded feldspars, and other minerals were converted to illite and K-feldspar. The diagenetic solutions probably were of continental origin and of low salinity because the Na/K values were sufficiently low to produce

only K-bearing silicate minerals (fig. 8). Fluvial sandstones sit unconformably on the profile, indicating a continental setting during burial.

Hekpoort Profile: Example of Early Diagenesis and Metasomatism.—The Hekpoort Basalt (2224 Ma) is widely developed in northern South Africa (Button 1979). It is disconformably overlain by coarse- to fine-grained clastic sedimentary rocks, dated at approximately 2095 Ma. The upper few meters of the basalt are interpreted (Button 1973) as an ancient residual clay soil formed 2200 Ma ago. More recently this profile has been reinterpreted by Retallack (1986) as having developed on a fining upward sequence of sandstone to shale derived from pre-existing soils developed on Hekpoort Basalt. This hinges largely on the interpretation of chamositic or "berthierine-rich" structures as sedimentary laminae. The remarkably consistent $TiO_2:Al_2O_3$ ratio throughout the Hekpoort profile does not seem consistent with the suggested fining upward sedimentary sequence. In either case, the profile is derived ultimately from weathering of the Hekpoort Basalt. The uppermost zone of the profile is Al-rich, containing abundant sericite, and andalusite where metamorphosed. Sericite, chlorite, quartz, and opaque minerals (probably Fe-oxides) are common in the profile (Button 1979). As
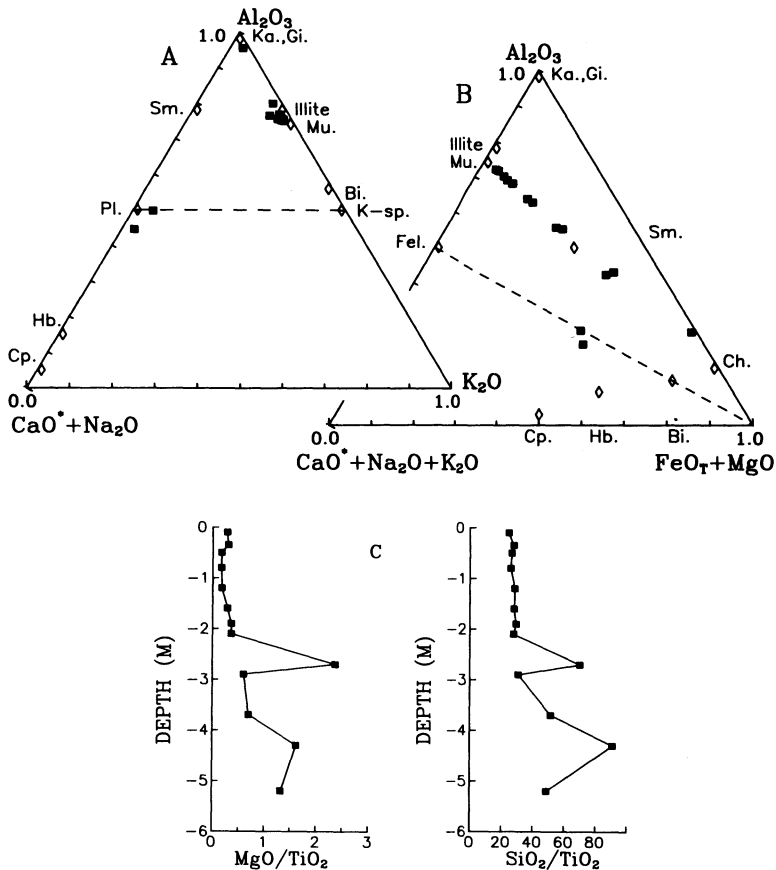
Fig. 10.—Analytical data for a weathering profile developed on the Early Proterozoic Hekpoort Basalt are shown on A-CN-K and A-CNK-FM plots in 10A and 10B (data from Button 1979). The data do not define any systematic trends such as those of Recent profiles. 10C illustrates the unusually high concentrations of some elements in the intermediate portion of the profile. They probably are a product of early diagenetic reactions.

in recent profiles (Wilson 1978), spheroidal weathering and original basaltic textures are preserved.

Anomalies and their explanation: Recent basaltic profiles contain abundant smectites in the lower, less weathered portions (Loughnan 1969), and the kandite group of minerals and/or gibbsite are dominant in the upper parts of mature profiles. The Hekpoort profile, in contrast, contains illite, chlorite, and quartz throughout. K_2O is low in basalts and ranges from 1 to 1.5% in the fresh Hekpoort basalts (Button 1979). Extremely weathered samples of the Hekpoort profile contain 8 to 10% K_2O. Comparable zones of recent profiles (Loughnan 1969; Patterson 1971) contain a few tenths of a percent K_2O and consist mainly of kaolinite and oxyhy-

droxides, rarely K-bearing minerals. Quartz is not present in the Hekpoort basalt, nor is it observed as a major authigenic phase in recent profiles, but it is a major constituent of the Hekpoort profile. Button (1979) argues that the profiles have been buried to a minimum depth of 15 km and suffered minimum burial temperatures of 300°C. The mineralogy of the profile probably reflects the effects of metasomatism and metamorphism.

The fresh Hekpoort basalt (Button 1979) plots where expected in A-CN-K space (fig. 10A), but unlike data from recent profiles (figs. 5, 6), no points plot along the left boundary (fig. 10A); one point plots at the Al_2O_3 apex, but the rest plot close to the illite composition (Fig. 10A), indicating that kaolinite and/or gibbsite produced during

weathering have been converted to illite. The reaction (eqn. 1) requires the introduction of K to the advanced zone of weathering (K-metasomatism) since little potash is present in the fresh basalt or would have been present in the profile (cf. Retallack 1986; Holland 1984; Curtis 1985).

In A-CNK-FM space, the Hekpoort data plot on a well-defined trend between illite and chlorite compositions (fig. 10*B*). The trend is dissimilar to the recent trends (figs. 5*B*, 6*B*) and cannot be explained by processes that affect recent profiles. The trend indicates that the Hekpoort profile consists of a mixture of illite (or compositionally equivalent sericite) and chlorite. The mineral assemblage does not change significantly, regardless of the weathering zone. In this respect the profile differs considerably from recent ones which have very well developed mineralogical zones.

The Hekpoort profile is most simply interpreted as an ancient weathering profile that was subjected to K-metasomatism and metamorphism. Introduction of potash resulted in the conversion weathering products (kaolinite and gibbsite?) to illite. The reaction is promoted by burial (increased temperature) and potassium probably has been introduced by solutions percolating along the initially porous and permeable weathering profile developed on the basalt. Subsequent metamorphism has produced a similar mineral assemblage in all weathering zones. Since the assemblages contain only a few mineral phases, equilibrium conditions would appear to have been approached or achieved. Potassium metasomatism suggests that continental waters probably were the agent of metasomatism.

Button (1979) suggests that a fluctuating water table intersected the weathering profile. The SiO_2/TiO_2 and MgO/TiO_2 ratios are plotted against depth in figure 10*C*. Anomalously high values for both ratios are noted in the middle and lower parts of the profile. There are no carbonates, but the trends are otherwise similar to those of the Murrurundi profile (fig. 7). In the recent Murrurundi profile, formation of montmorillonite accounts for the accumulation of SiO_2 and MgO (relative to TiO_2). A similar origin is likely for these oxides in the Hekpoort profile. Subsequent metamorphism con-

verted montmorillonite to the stable (high temp.) assemblage of chlorite and quartz. Note that even in the Murrurundi profile, where SiO_2 accumulates in the perched ground water zone, no quartz forms. Other siliceous minerals, primarily montmorillonite, take up silica.

Butler Hill Profile: Example of Na-Metasomatism and Physical Segregation.— The Butler Hill Granite is dated at 1185 Ma old. It contains 35% modal quartz, 5% biotite, and plagioclase and perthitic alkali feldspar in subequal amounts (Blaxland 1974). The granite is unconformably overlain by the Cambrian, marine, Lamotte Sandstone. Below the unconformity there is a 20 m-thick weathering profile. Field relations and isotopic data (Blaxland 1974) indicate that the profile was developed during the Proterozoic.

Anomalies and interpretation: The data of Blaxland (1974) are plotted on the A-CN-K and A-CNK-FM diagrams (fig. 11*A*, 11*B*). The trends are atypical of granitic weathering profiles. Two samples plot close to the plagioclase position. These samples are in the zones of incipient and intermediate weathering. They contain 6.92 and 8.92 wt% soda whereas CaO is 0.34 and 0.26 and K is 0.61 and 1.93. Soda is 3.46 wt% in the unweathered rock. Na has been added to the profile as albite. There is no evidence that the profile was subjected to high temperatures (above approx. 250°C). Na-metasomatism may have occurred during marine transgression that deposited the Lamotte Sandstone and during subsequent burial.

SUMMARY AND DISCUSSION

Chemical weathering of common minerals such as feldspars, amphiboles, pyroxenes, and phyllosilicates produces only a few *abundant* groups of secondary minerals, primarily the kandites, smectites, and illites. The clay minerals commonly develop preferentially after specific primary minerals; consequently the secondary mineralogy of weathering profiles is dependent upon both the primary mineralogy and its distribution in the parent rock. In many situations it is difficult to differentiate parent and daughter products, or to assess the alteration sequence in a mature weathering profile, by studying mineralogy alone. Dependence of such studies on X-ray
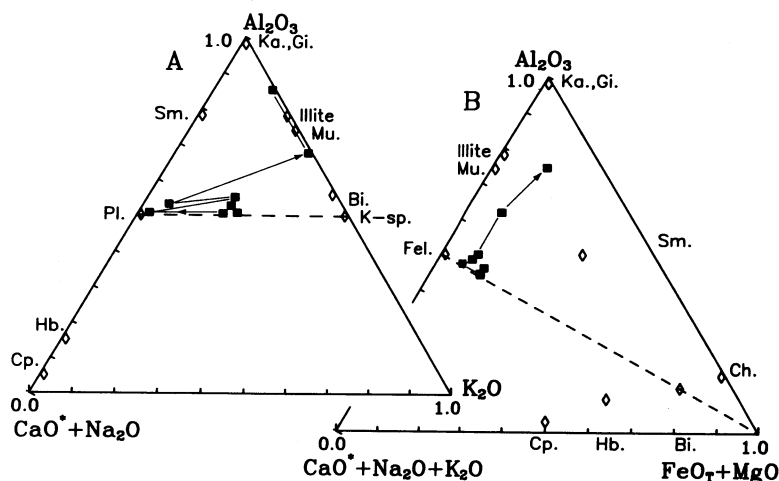
FIG. 11.—Analytical data for a weathering profile developed on the Butler Hill Granite are plotted (data from Blaxland 1974). The lines connect progressively shallower samples to illustrate the enrichment of some samples in Na. The trends are different from trends developed in Recent weathering profiles on granites and indicate Na-metasomatism of parts of the profile. 11C illustrates Al_2O_3/TiO_2 of the samples.

diffraction methods exacerbates the problems because the data are semi-quantitative. Although mature weathering profiles are mineralogically complex, we have attempted to demonstrate that the bulk compositions follow simple trends that are largely unaffected by climatic conditions under which weathering proceeded. The alkali and alkaline earth elements are leached from the profile in preference to elements such as Ti, Fe^{3+}, and Al. Recent profiles developed from volcanic and plutonic rocks of diverse composition display systematic, predictable, compositional weathering trends (fig. 3). Complications include physical processes (infiltration of fines and winnowing) and diagenetic reactions (ground water interactions with the profiles). If weathering processes and mechanisms have always been similar, then trends observed in paleosols can be interpreted by comparison with trends of recent profiles and predicted trends.

Chemical studies of some paleosols indicate that they have been affected significantly by diagenetic reactions, including K-, Mg-, Fe-, or Na-metasomatism. Kaolinite has been converted to illite and chlorite. Partially degraded feldspars of the incipiently weathered zones have been converted to either K-feldspar or albite. These are "late" diagenetic effects. There is evidence of early diagenetic effects in some of the paleosols. The Hekpoort and Boulder Creek profiles contain evidence of reaction with perched or permanent ground water. Features preserved in these paleosols help to evaluate ancient climates and paleogeographic settings.

REFERENCES CITED

ALTSCHULER, Z. S.; DWORNIK, E. J.; and KRAMER, H., 1963, Transformation of montmorillonite to kaolinite during weathering: Science, v. 141, p. 148–152.

BAIN, D. C., 1972, Oxidation of chlorites in soil clays and effect on DTA curves: Nature, v. 238, p. 142–143.

————, 1977, The weathering of ferruginous chlorite in a podzol from Argyllshire, Scotland: Geoderma, v. 17, p. 193–208.

————; RITCHIE, P. F. S.; CLARK, D. R.; and DUTHIE, D. M. L., 1980, Geochemistry and mineralogy of weathered basalt from Morvern, Scotland: Mineral. Mag., v. 43, p. 865–872.

BERNER, R. A., and HOLDREN, G. R., 1979, Mechanism of feldspar weathering-II. Observations of feldspars from soils: Geochim. Cosmochim. Acta, v. 43, p. 1173–1186.

BLATT, H., 1979, Diagenetic processes in sandstones, *in* SCHOLLE, P. A., and SCHLUGER, P. R.,

eds., Aspects of diagenesis: SEPM Spec. Pub. 26, p. 141–157.

——, and JONES, R. L., 1975, Proportions of exposed igneous, metamorphic, and sedimentary rocks: Geol. Soc. America Bull., v. 86, p. 1085–1088.

BLAXLAND, A. B., 1974, Geochemistry and geochronology of chemical weathering, Butler Hill Granite, Missouri: Geochim. Cosmochim. Acta, v. 38, p. 843–852.

BROCK, R. W., 1943, Weathering of igneous rocks near Hong Kong: Geol. Soc. America Bull., v. 54, p. 717–738.

BUSENBERG, E., and CLEMENCY, C. V., 1976, The dissolution kinetics of feldspars at 25°C and 1 atm CO_2 partial pressure: Geochim. Cosmochim. Acta, v. 40, p. 41–49.

BUTTON, A., 1973, A regional study of the stratigraphy and development of the Transvaal Basin in eastern and northeastern Transvaal: Unpub. Ph.D. thesis, Univ. of Witswatersrand, Johannesburg, SA., 352 p.

——, 1979, Early Proterozoic weathering profile on the 2200 m.y. old Hekpoort Basalt, Pretoria Group, South Africa: Geol. Res. Unit, Info. Circ. 133, Johannesburg, SA., 19 p.

CLARKE, F. W., 1924, The data of geochemistry: U.S. Geol. Surv. Prof. Paper, 770, 841 p.

CLAUER, N., 1981, Strontium and argon isotopes in naturally weathered biotites, muscovites, and feldspars: Chem. Geol., v. 31, p. 325–334.

——; O'NEIL, J. R.; and BONNOT-COURTOIS, C., 1982, The effect of natural weathering on the chemical and isotopic compositions of biotites: Geochim. Cosmochim. Acta, v. 46, p. 1755–1762.

CORRENS, C. W., 1940, Die chemische verwitterung der silicate: Naturvissen, v. 28, p. 369–373.

CRAIG, D. C., and LOUGHNAN, F. C., 1964, Chemical and mineralogical transformations accompanying the weathering of basic volcanic rocks from New South Wales: Aust. Jour. Soil Res., v. 2, p. 218–234.

DUDDY, I. R., 1980, Redistribution and fractionation of rare-earth and other elements in a weathering profile: Chem. Geol., v. 30, p. 363–381.

ELLIS, A. J., and MAHON, W. A. J., 1967, Natural hydrothermal systems and experimental hot water/rock interactions (part II): Geochim. Cosmochim. Acta, v. 31, p. 519–538.

FEAKES, C. R., and RETALLACK, G. J., 1988, Recognition and chemical characterization of fossil soils developed on alluvium: a Late Ordovician example, in REINHARDT, J., and SIGLIO, W. R., eds., Paleosols and weathering through time: principles and applications: Geol. Soc. America Spec. Paper 216, p. 35–48.

GARRELS, R. M., and MACKENZIE, F. T., 1967, Origin of the chemical compositions of some springs and lakes, in GOULD, R. F. ed., Equilibrium Concepts in Natural Water Systems: Amer. Chem. Soc. Adv. Chem. Series 67, p. 222–242.

GAY, A. L., and GRANDSTAFF, D. E., 1980, Chemistry and mineralogy of Precambrian paleosols at Elliot Lake, Ontario, Canada: Precamb. Res., v. 12, p. 349–373.

GRAF, D. L.; MEENTS, W. F.; FRIEDMAN, I.; and SHIMP, N. F., 1966a, The origin of saline formation waters, III: calcium chloride waters: Illinois Geol. Surv. Circ. 397, 60 p.

GRANT, W. H., 1963, Weathering of Stone Mountain Granite, in INGERSOL, E., ed., Clays and Clay Minerals: Oxford, Pergamon, p. 65–73.

HABERMEHL, M. A., 1980, The Great Artesian Basin, Australia: Aust. Jour. Geol. and Geophysics, v. 5, p. 9–38.

HELGESON, H. C., 1969, Thermodynamics of hydrothermal systems at elevated temperatures and pressures: Am. Jour. Sci., v. 267, p. 729–804.

——, 1971, Kinetics of mass transfer among silicates and aqueous solutions: Geochim. Cosmochim. Acta, v. 35, p. 421–469.

——; DELANEY, J. M.; NESBITT, H. W.; and BIRD, D. K., 1978, Summary and critique of the thermodynamic properties of rock-forming minerals: Am. Jour. Sci., v. 278-A, pp. 1–229.

——; GARRELS, R. M.; and MACKENZIE, F. T., 1969, Evaluation of irreversible reactions in geochemical processes involving minerals and aqueous solutions—II: Geochim. Cosmochim. Acta, v. 33, p. 455–481.

HITCHON, B.; BILLINGS, G. K.; and KLOVAN, J. E., 1971, Geochemistry and origin of formation waters in the western Canada sedimentary basin—III. Factors controlling chemical composition: Geochim. Cosmochim. Acta, v. 35, p. 567–598.

HOLDREN, G. R., and BERNER, R. A., 1979. Mechanism of feldspar weathering—I: Geochim. Cosmochim. Acta, v. 43, p. 1161–1172.

HOLLAND, H. D., 1984, The Chemical Evolution of the Atmosphere and Oceans: Princeton, NJ, Princeton Univ. Press, 582 p.

KRONBERG, B. I.; FYFE, W. S.; LEONARDOS, O. H., JR.; and SANTOS, A. M., 1979, The chemistry of some Brazilian soils: element mobility during intense weathering: Chem. Geol., v. 24, p. 211–229.

——, and NESBITT, H. W., 1981, Quantification of weathering, soil geochemistry and soil fertility: Jour. Soil Sci., v. 32, p. 453–459.

LASAGA, A. C., 1984, Chemical kinetics of water-rock Interactions: Jour. Geophys. Res., v. 89, p. 4009–4025.

LAWRENCE, C. R., 1975, Geology, hydrodynamics, and hydrochemistry of the southern Murray Basin: Geol. Surv. Victoria Mem. 30, 359 p.

LIVINGSTONE, D. A., 1963, Chemical composition of rivers and lakes: U.S. Geol. Surv. Prof. Paper 440-G, 64 p.

LOUGHNAN, F. C., 1969, Chemical Weathering of Silicate Minerals: London, Elsevier, 155 p.

LOVERING, T. S., 1959, Significance of accumulator plants in rock weathering: Geol. Soc. America Bull., v. 70, p. 781–800.

MARKOVICS, G., 1977, Chemistry of weathering of the Toorongo Granodiorite, Mt. Baw Baw Vic: Unpub. Honours Thesis, La Trobe Univ., Victoria, Aust., 36 p.

MELFI, A. J.; CERRI, C. C.: KRONBERG, B. I.; FYFE, W. S.; and McKINNON, B., 1983, Granitic weathering: a Brazilian study: Jour. Soil Sci., v. 34, p. 841–851.

MEUNIER, A., and VELDE, B., 1976, Mineral reactions at grain contacts in early stages of granite weathering: Clay Minerals, v. 11, p. 235–240.

MINARIK, L.; ABSOLON, K.; ZDISLAVA, K.; and KLECKA, M., 1983, Chemical changes of granite during its weathering, in AUGUSTITHIS, S. S., ed., Leaching and Diffusion in Rocks and their Weathering Products: Athens, Theophrastus, p. 293–306.

NESBITT, H. W., 1977, Estimation of the thermodynamic properties of Na- Ca- and Mg-beidellites: Can. Mineral., v. 15, p. 22–30.

————, 1979, Mobility and fractionation of rare earth elements during weathering of a granodiorite: Nature, v. 279, p. 206–210.

————; MARKOVICS, G.; and PRICE, R. C., 1980, Chemical processes affecting alkalies and alkaline earths during continental weathering: Geochim. Cosmochim. Acta, v. 44, p. 1659–1666.

————, and YOUNG, G. M.,1982, Early Proterozoic climates and plate motions inferred from major element chemistry of lutites: Nature, v. 299, p. 715–717.

————, and ————, 1984, Prediction of some weathering trends of plutonic and volcanic rocks based on thermodynamic and kinetic considerations: Geochim. Cosmochim. Acta, v. 48, p. 1523–1534.

NOCKOLDS, S. R., 1954, Average chemical compositions of some igneous rocks: Geol. Soc. America Bull., v. 65, p. 1007–1032.

NOVIKOFF, A.; TSAWLASSOU, G.; GAC, J. Y.; BOURGEAT, F.; BOULET, R.; and TARDY, Y., 1972, Alteration des biotites dans les arenes des pays temperes, tropicaux et equatoriaux: Sci. Geol. Bull. Strasbourg, v. 25, p. 287–306.

PACES, T., 1972, Chemical characteristics and equilibration in natural water-felsic rock-CO$_2$ system: Geochim. Cosmochim. Acta, v. 36, p. 217–240.

————, 1973, Steady-state kinetics and equilibrium between ground water and granitic rock: Geochim. Cosmochim. Acta, v. 37, p. 2641–2663.

————, 1983, Rate constants of dissolution derived from the measurements of mass balance in hydrological catchments: Geochim. Cosmochim. Acta, v. 47, p. 1855–1864.

PATTERSON, S. H., 1971, Investigations of ferruginous bauxite and other mineral resources of Kauai and a reconnaissance of ferruginous bauxite deposits on Maui, Hawaii: U.S. Geol. Surv. Prof. Paper 656, 65 p.

PETROVIC, R., 1976, Rate control in feldspar dissolution: II. The protective effect of precipitates: Geochim. Cosmochim. Acta, v. 40, p. 1509–1522.

————, 1981a, Kinetics of dissolution of mechanically comminuted rock-forming oxides and silicates—I. Deformation and dissolution of quartz under laboratory conditions: Geochim. Cosmochim. Acta, v. 45, p. 1665–1674.

————, 1981b, Kinetics of dissolution of mechanically comminuted rock-forming oxides and silicates—II. Deformation and dissolution of oxides and silicates in the laboratory and at the Earth's surface: Geochim. Cosmochim. Acta, v. 45, p. 1675–1686.

————; BERNER, R. A.; and GOLDHABER, M. B., 1976, Rate control in dissolution of alkali feldspars—I. Study of residual feldspar grains by X-ray photoelectron spectroscopy: Geochim. Cosmochim. Acta, v. 40, p. 537–548.

PETTIJOHN, F. J., 1975, Sedimentary Rocks: New York, Harper and Row, 628 p.

ROBERT, M., 1970, Etude experimentale de la desegregation du granite et de l'evolution des micas: These Sci., Univ. Paris, 194 p.

ROSS, G. J., 1975, Experimental alteration of chlorites into vermiculites by chemical oxidation: Nature, v. 255, p. 133–134.

SAND, L. B., and BATES, T. L., 1953, Mineralogy of the residual kaolins of the Southern Appalachians: Am. Mineral., v. 38, p. 358–372.

SCHAU, M., and HENDERSON, J. B., 1984, Archean chemical weathering at three localities in the Canadian Shield: Precamb. Res., v. 20, p. 189–224.

SINGER, A., 1980, The paleoclimatic Interpretation of clay minerals in soils and weathering profiles: Earth Sci. Rev., v. 15, p. 303–326.

STEPHENS, M. B.; GLASSON, M. J.; and KEAYS, R. R., 1979, Structural and chemical aspects of metamorphic layering development in metasediments from Clunes, Australia: Am. Jour. Sci., v. 279, p. 129–160.

TOTH, J., 1962, A theoretical analysis of groundwater flow in small drainage basins: Third Canad. Hydrology Symposium, Calgary, p. 75–96.

TSAWLASSOU, G., 1971, Geochimie de l'alteration des roches granitiques et gneissiques en pays tropical et equatorial. Evolution des biotites et des feldspaths: These 3e cycle, Univ. Strasbourg, 68 p.

WAHLSTROM, E. E., 1948, Pre-Fountain and recent weathering on Flagstaff Mountain near Boulder, Colorado: Geol. Soc. America Bull., v. 59, p. 1173–1190.

WEAVER, C. E., 1967, Potassium, illite, and the oceans: Geochim. Cosmochim. Acta, v. 31, p. 281–296.

————, and POLLARD, L. D., 1973, The Chemistry of Clay Minerals: Amsterdam, Elsevier, 213 p.

WHITE, A. F., 1983, Surface chemistry and dissolution kinetics of glassy rocks: Geochim. Cosmochim. Acta, v. 47, p. 805–816.

————; CLAASSEN, H. C.; and BENSON, L. V., 1980, The effect of dissolution of volcanic glass on the water chemistry in a tuffaceous aquifer, Rainier Mesa, Nevada: U.S. Geol. Surv. Water-Supply Paper 1535-Q, 34 p.

WHITE, D. W.; HEM, J. D.; and WARING, G. A., 1963, The chemical composition of subsurface waters: U.S. Geol. Surv. Prof. Paper 440-F, 67 p.

WILSON, R. E., 1978, Mineralogy, petrology, and geochemistry of basalt weathering: Unpub. Honours Thesis, Latrobe Univ. Victoria, Aust., 55 p.

WOLLAST, R. 1967, Kinetics of the alteration of K-feldspar in buffered solutions at low temperature: Geochim. Cosmochim. Acta, v. 31, p. 635–648.